Preparation of an IGRF-14 geomagnetic field model candidate (C^3FM4)

Ingo Wardinski*[1]

[1]EOST Strasbourg, France

October 1, 2024

1 Data

+ the parent model covers the period 1956.5 to 2025.1,
+ model is based on annual differences derived from observatory monthly means,
+ monthly means are derived from most recent WDC and IMO data sets (hourly means and minute means, respectively)
+ total number of data is 306774

2 Modelling strategy

+ classical spline modeling, where the temporal variability is parameterized using order 6 B-splines, $\ell_{\max} = 14$ and a spline knot-spacing ~ 1.4 years
+ model is constrained in time and space, also the second time derivative is controlled at the model endpoints,
+ model is constraint to fit a satellite based main field model (Lesur et al.,2020) in 2019
+ forecasting secular variation using a multivariate singular-spectrum-analysis (SSA) of the 80 secular variation coefficients,
+ forecasts are based on the secular variation from 1960 to 2023 and start at 2023.0, we choose this setting to avoid edge effects from loosely constrained secular acceleration at both end points.

*wardinski@unistra.fr

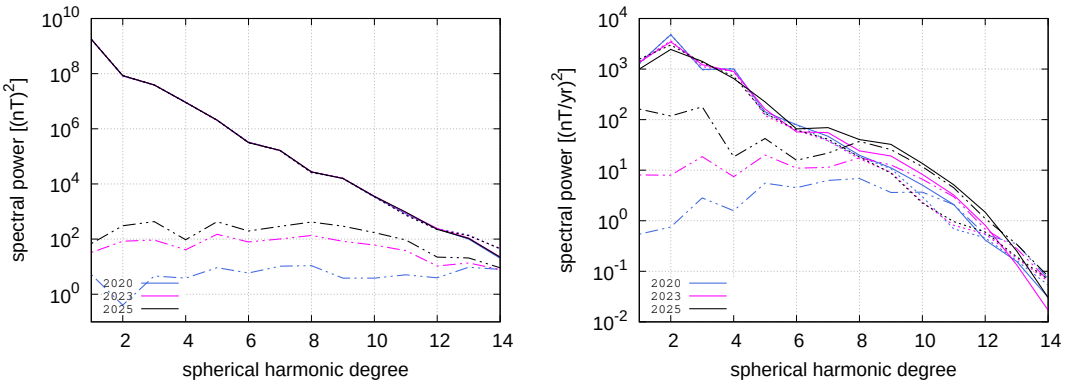

Figure 1: Spectra of main field models of C^{3}FM4 (solid lines) and Chaos 7.18 (dotted lines) at different epochs, right for the secular variation models. Dash-dotted lines represent respective spectra of the differences.

3 Candidates

+ a DGRF candidate is derived for the epoch 2020.0
+ an IGRF candidate is derived for the epoch 2025.0
+ a SV candidate for the period 2025 - 2030 is derived from secular variation model centered at the epoch 2027.5

4 Initial comparisons of main field and secular variation models

Figure 2 shows the degree correlation derived between main field models of Chaos 7.18 and C^{3}FM4 and their secular variations. Main field models appear to be similar. Their spectra and those of their differences do not intersect for $\ell_{\max} < 15$

Figures 3 and 4 show comparisons between modeled and observed secular variation at different ground-based observatory sites. Again, we compare Chaos7.18 and two branches of the C^{3}FM4.

The candidate for the epoch are derived from the spline model, but not from forecasts based on a multivariate SSA. The very reason for this is the termination of the forecasts after $\ell_{\max} = 8$.

5 Comparisons of secular variation forecasts

Forecasts of the two first secular variation coefficients show different slopes and temporal complexity, Figures 5 and 6. Most distinguishable are forecasts based on ten eigenmodes of the multivariate SSA (plots second row left), which is a strong weakening of the secular

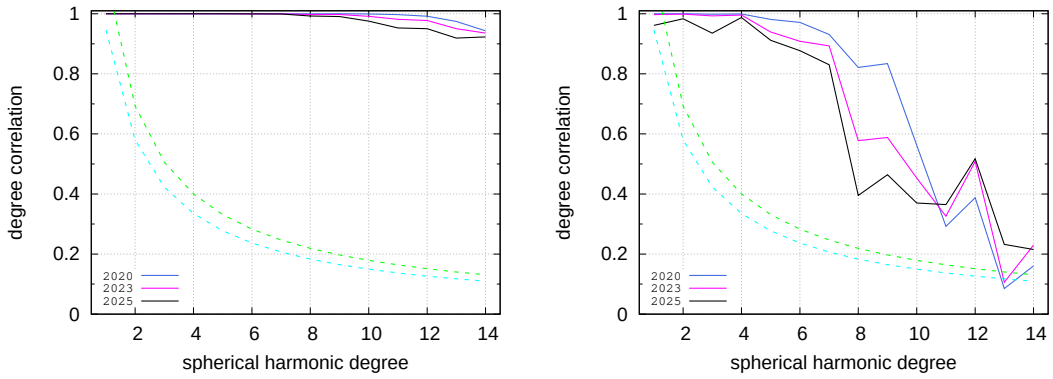

Figure 2: Degree correlation derived between the models of C^{3}FM4 and Chaos 7.18. Left, for the main field. The right panel shows similarly degree correlation for the secular variation at three different epochs. The dashed lines refer to levels of 95% and 90% significance, respectively.

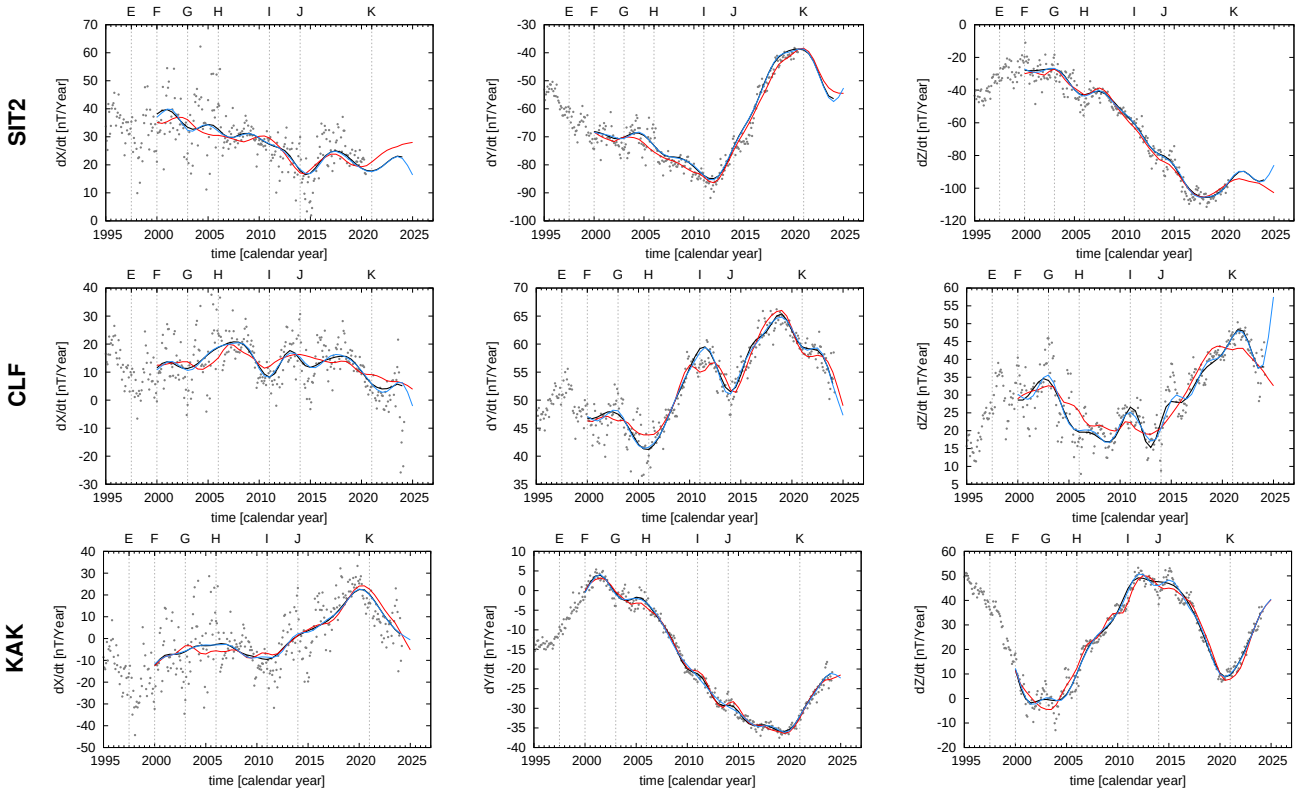

Figure 3: Plot of the secular variation components at different observatory sites, Chaos7.18 - red, light blue - candidate parent (C^{3}FM4), black - C^{3}FM4 terminated at 2024.1. Letters indicate known geomagnetic jerks.

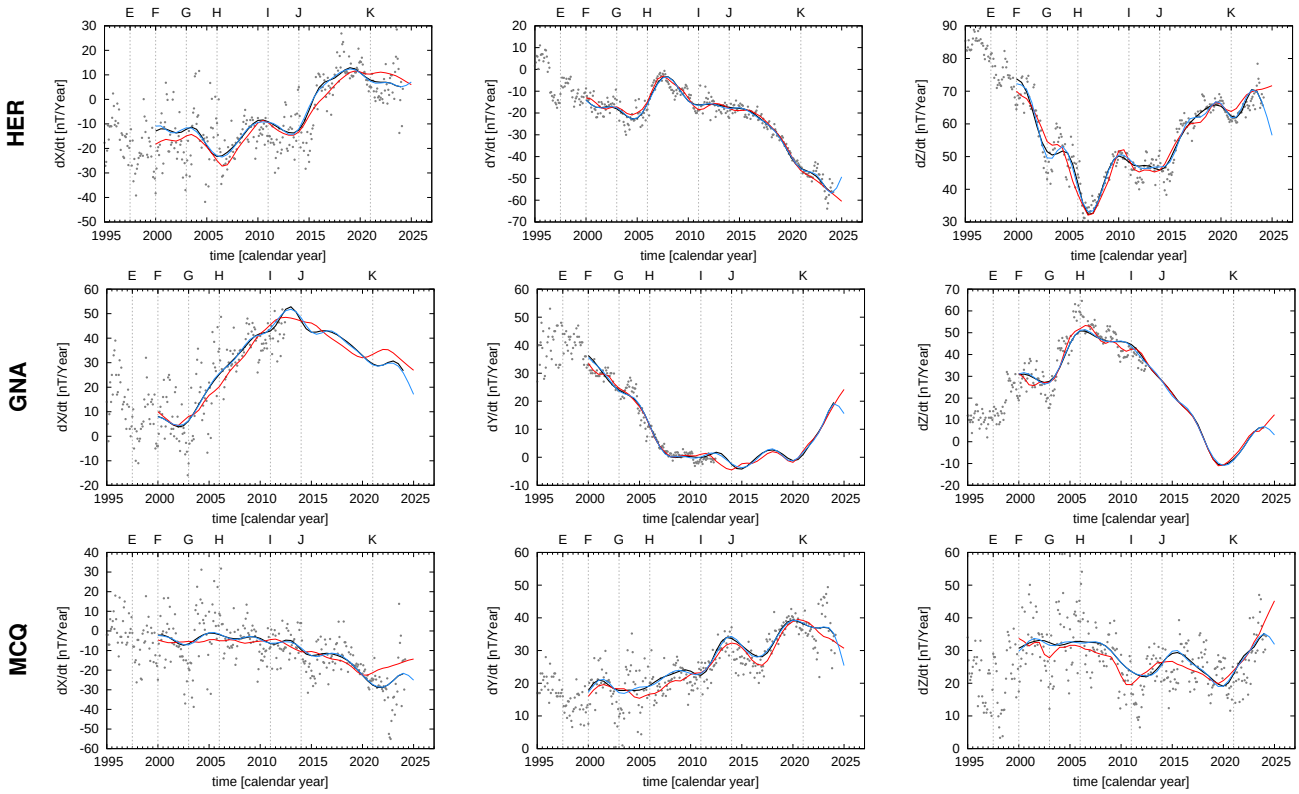

Figure 4: Plot of the secular variation components at different observatory sites, Chaos7.18 - red, light blue - candidate parent (C^3FM4), black - C^3FM4 terminated at 2024.1. Letters indicate known geomagnetic jerks.

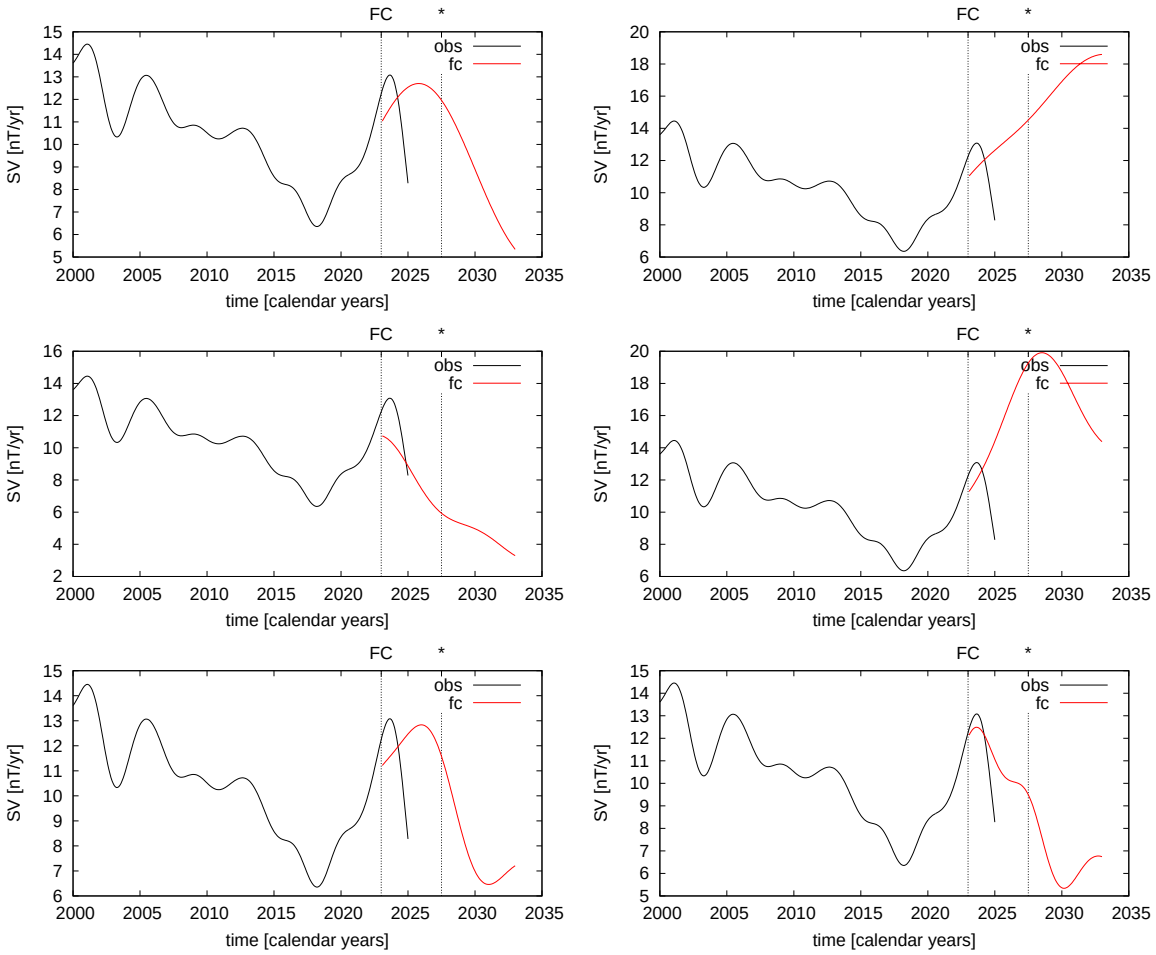

Figure 5: Plot of secular variation forecasts of g_1^0, for different numbers of eigenmodes, i.e. 8, 9, 10, 12, 14 and 20.

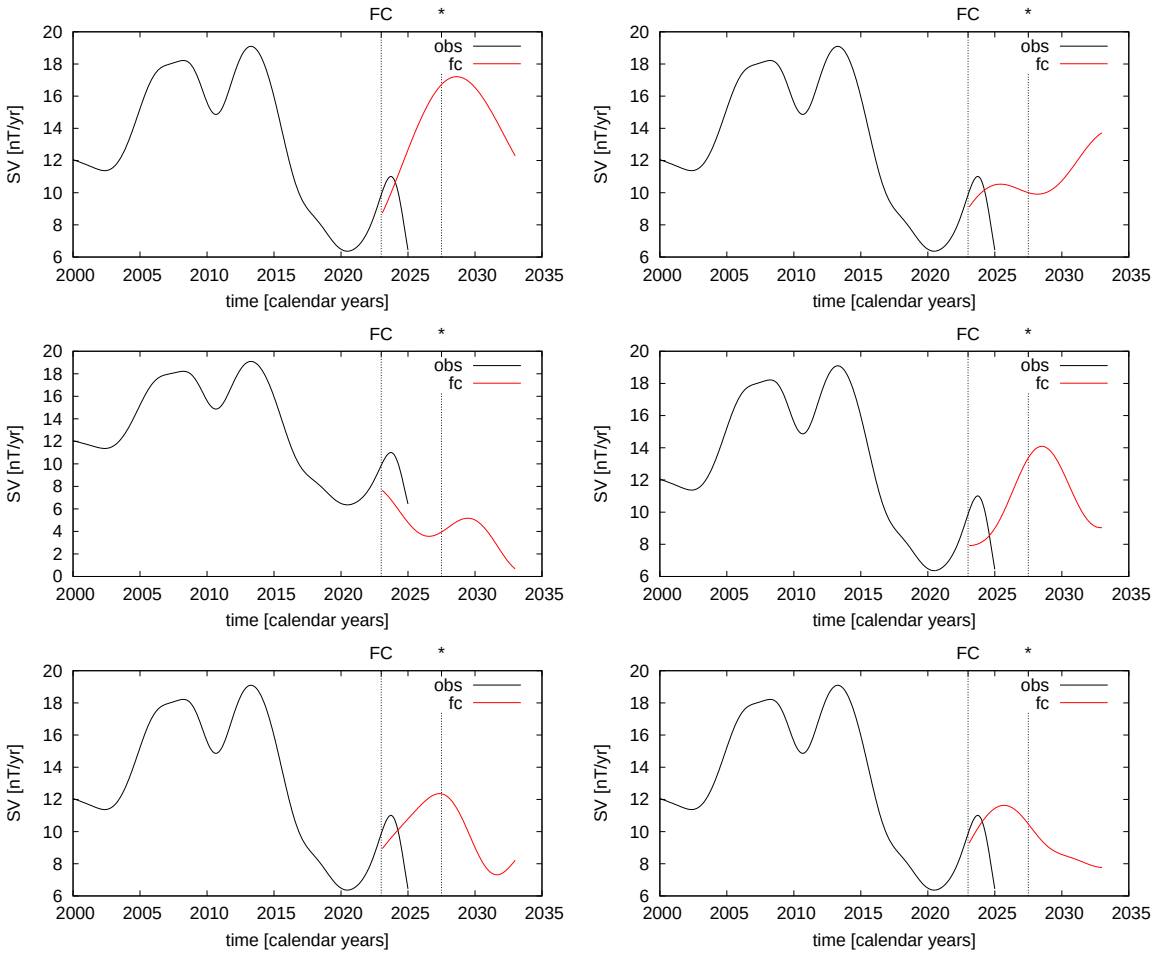

Figure 6: Plot of secular variation forecasts of g_1^1, for different numbers of eigenmodes, i.e. 8, 9, 10, 12, 14 and 20..

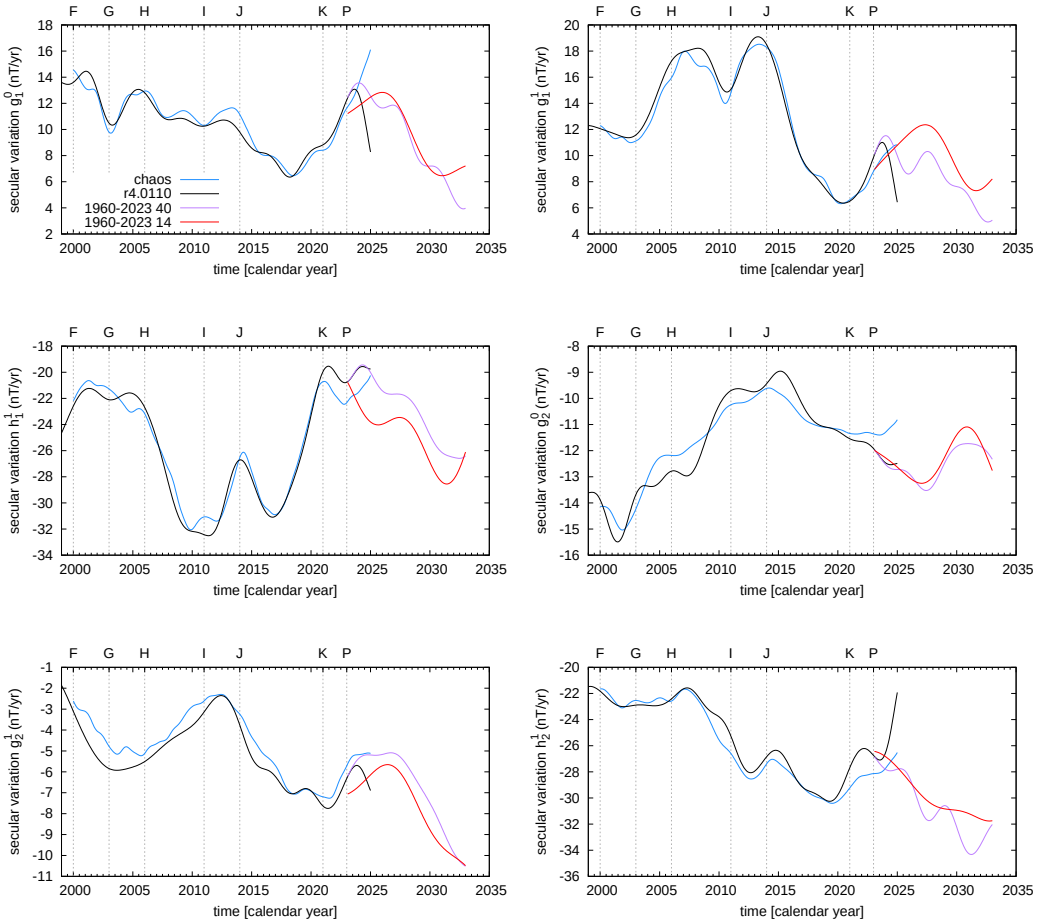

Figure 7: Plot of the first six secular variation coefficients, Chaos7.18 - light blue, our candidate - black, the forecast candidate - red and another (more complex) forecast - purple. Letters F-K indicate known geomagnetic jerks, P (at 2023) indicates the beginning of the prediction phase.

variation. A straight strengthening of g_1^0 secular variation is only displayed by using 9 eigenmodes (Figure 5 top right). All other forecasts show a belly-type behavior. We favor forecasts based on 14 eigenmodes of the multivariate SSA (Figures 5 and 6 bottom left).

6 Initial interpretation

The degree correlation highlight only minor differences between the MF models of Chaos 7.18 and C^{3}FM4 for epochs after 2020. The differences slightly reduce when C^{3}FM4 is constrained to fit a satellite-based main field model in 2019, rather than in 2015. At maximum, these models can be considered matching each other to spherical harmonic degree $\ell = 12 - 14$ with a correlation ~ 0.9 .

The degree correlation of the secular variation differ substantially. This can be explain

by the apparent differences of the secular variation. However, the constraint to fit a main field model at any epoch for spherical harmonic degrees $\ell = 7 - 14$. The simplest explanation would be that ground-based and satellite-based secular variation models differ, because of their different source geometries. Satellite data consider every magnetic field generation below their orbital sphere to be of internal origin. However, this might be difficult as night-time and quiet-time ionospheric field generation may also map into these data as internal sources. An indication for this might be the higher power of ground-based secular variation models for spherical harmonic degrees $\ell = 4 - 12$, Figure 1.

Plots of the secular variation coefficients (Figures 7, 5 and 6) show a strong oscillation towards the end point. This is related to end point constrain in the inversion, which may not be functioning properly. However, this seems to be reflected in the degree correlation, which may indicate a similar problem in the derivation of Chaos 7.18.

References